Interaction of Triphenyltin Hydride and Rhodium. Structure of $[Rh(NCBPh_3)(H)(SnPh_3)(PPh_3)_2]$ and NMR (^1H, ^{15}N, ^{31}P, ^{103}Rh, ^{119}Sn) Study of Pyridine-Containing Derivatives

Laurence Carlton,* Rosemarie Weber, and Demetrius C. Levendis

Centre for Molecular Design, Department of Chemistry, University of the Witwatersrand, Johannesburg, Republic of South Africa

Received May 30, 1997

The structure of $[Rh(NCBPh_3)(H)(SnPh_3)(PPh_3)_2]$ (**1**) (formed from $[Rh(NCBPh_3)(PPh_3)_3]$ and Ph_3SnH) was determined by a single-crystal X-ray diffraction study which shows the geometry to be equally well described as a distorted tetragonal pyramid with tin at the apex or a distorted trigonal bipyramid with a hydrogen of one of the phosphine phenyl groups occupying the sixth coordination site. The tin-hydride distance of 2.31(5) Å is consistent with a weak interaction. Crystal data for **1**: space group, $P2_1/c$; $a = 12.564(4)$, $b = 26.942(4)$, $c = 18.000(3)$ Å; $\beta = 92.93(2)°$; $V = 6085(2)$ Å^3; $Z = 4$; $R = 0.050$ for 5655 reflections with $I \geq 2\sigma(I)$. Complex **1** reacts with pyridine and substituted pyridines L (L = pyridine (py) (**a**), 4-(dimethylamino)pyridine (4-Me_2Npy) (**b**), and 4-carbomethoxypyridine (4-MeO_2Cpy) (**c**)) in dichloromethane at −25 °C to give *trans*-$[Rh(NCBPh_3)(H)(SnPh_3)(PPh_3)_2(L)]$ (**2a**−**c**). With L = 4-Me_2Npy, the products *cis*-$[Rh(NCBPh_3)(H)(SnPh_3)(PPh_3)_2(4\text{-}Me_2Npy)]$ (**3**) and *cis*- and *trans*-$[Rh(NCBPh_3)(H)(SnPh_3)(PPh_3)(4\text{-}Me_2Npy)_2]$ (**4** and **5**, respectively) are also formed. At room temperature, $[Rh(NCBPh_3)(H)(SnPh_3)(PPh_3)(L)]$ (**6a**−**c**) is the final product, decomposing over a period of hours. The pyridine-containing complexes were not isolated and were characterized by NMR spectroscopy, which showed the magnitude of the spin coupling constant J(Sn−H) to increase by factors of up to 5.5 compared with the value of 29 Hz observed for **1**. At 50 °C, **6** (in the presence of L and PPh_3 originating from **1**) undergoes reductive elimination of Ph_3SnH to give *cis*-$[Rh(NCBPh_3)(PPh_3)_2(L)]$; at this temperature **1** is stable, decomposing only at temperatures of 85 °C and above. A kinetic study of the dissociation of Ph_3SnH from **6b** (L = 4-Me_2Npy) gave activation parameters $\Delta H^{\ddagger} = 97 \pm 6$ kJ mol^{-1} and $\Delta S^{\ddagger} = 1 \pm 20$ J K^{-1} mol^{-1}. The weakened interaction between Ph_3SnH and rhodium is accounted for in terms of a three-center "agostic" bond.

Introduction

The generally accepted view that a three-center "agostic" interaction occurs during the activation of alkanes by transition metals is based on structural studies of a wide range of examples in which oxidative addition is incomplete.[1] This type of bonding is also found with organosilicon[2] and organotin[3] analogues where the unsupported R_3EH−transition metal bond (E = Si, Sn) is more stable and more readily characterized. The three-center R_3SiH−metal interactions are of interest as models for alkane binding and intermediates in hydrosilylation catalysis;[4] those involving tin show apparently enhanced reactivity of R_3-Sn, having been implicated in the facile derivatization of the cyclopentadienyl ligand of $[Co(Cp)(CO)_2]$.[5]

Accurate location by X-ray diffraction of the hydrogen in such systems is not easy, and few neutron studies have been reported.[6] A means of identifying such activated bonding modes that does not rely on diffraction methods is desirable since, by their nature, the majority of such systems are not amenable to crystallographic study. NMR spectroscopy, although well suited to the detection of unstable and reactive species in solution, suffers from the drawback that the parameter of greatest utility in the characterization of R_3EH−transition metal interactions, namely the E−H spin coupling constant, is a function of a number of variables not all related to the strength of the E−H bond. For this reason, an independent measure of the strength of either the E−H or the R_3EH−transition metal bond is an important means of validating the use of J(E−H) as an indicator of such interactions in systems observed in solution. We report

(1) (a) Brookhart, M.; Green, M. L. H. *J. Organomet. Chem.* **1983**, *250*, 395. (b) Muetterties, E. L. *Chem. Soc. Rev.* **1982**, *11*, 283. (c) Brookhart, M.; Green, M. L. H.; Wong, L.-L. *Prog. Inorg. Chem.* **1988**, *36*, 1. (d) Crabtree, R. H.; Hamilton, D. G. *Adv. Organomet. Chem.* **1988**, *28*, 299. (e) Crabtree, R. H. *Angew. Chem., Int. Ed. Engl.* **1993**, *32*, 789.

(2) (a) Graham, W. A. *J. Organomet. Chem.* **1986**, *300*, 81. (b) Schubert, U. *Adv. Organomet. Chem.* **1990**, *30*, 151. (c) Luo, X.-L.; Kubas, G. J.; Bryan, J. C.; Burns, C. J.; Unkefer, C. J. *J. Am. Chem. Soc.* **1994**, *116*, 10312; **1995**, *117*, 1159. (d) Jagirdar, B. R.; Palmer, R.; Klabunde, K. J.; Radonovich, L. J. *Inorg. Chem.* **1995**, *34*, 278.

(3) (a) Schubert, U.; Kunz, E.; Harkers, B.; Willnecker, J.; Meyer, J. *J. Am. Chem. Soc.* **1989**, *111*, 2572. (b) Piana, H.; Kirchgässner, U.; Schubert, U. *Chem. Ber.* **1991**, *124*, 743. (c) Schubert, U.; Gilbert, S.; Mock, S. *Chem. Ber.* **1992**, *125*, 835.

(4) (a) Colomer, E.; Corriu, R. J. P.; Marzin, C.; Vioux, A. *Inorg. Chem.* **1982**, *21*, 368. (b) Carré, F.; Colomer, E.; Corriu, R. J. P.; Vioux, A. *Organometallics* **1984**, *3*, 1272.

(5) Carlton, L.; Maaske, B. *J. Organomet. Chem.* **1994**, *468*, 235.

(6) (a) Schultz, A. J.; Williams, J. M.; Schrock, R. R.; Rupprecht, G. A.; Fellmann, J. D. *J. Am. Chem. Soc.* **1979**, *101*, 1593. (b) Brown, R. K.; Williams, J. M.; Schultz, A. J.; Stucky, G. D.; Ittel, S. D.; Harlow, R. L. *J. Am. Chem. Soc.* **1980**, *102*, 981. (c) Beno, M. A.; Williams, J. M.; Tachikawa, M.; Muetterties, E. L. *J. Am. Chem. Soc.* **1981**, *103*, 1485. (d) Schultz, A. J.; Teller, R. G.; Beno, M. A.; Williams, J. M.; Brookhart, M.; Lamanna, W.; Humphrey, M. B. *Science* **1983**, *220*, 197. (e) Schubert, U.; Ackermann, K.; Wörle, B. *J. Am. Chem. Soc.* **1982**, *104*, 7378. (f) Schubert, U.; Scholz, G.; Müller, J.; Ackerman, K.; Wörle, B.; Stansfield, R. F. D. *J. Organomet. Chem.* **1986**, *306*, 303.

S0020-1669(97)00662-9 CCC: $15.00
Published on Web 02/24/1998

the results of a study of triphenyltin hydride complexes of rhodium which seeks to address this matter.

Experimental Section

$[Rh(NCBPh_3)(H)(SnPh_3)(PPh_3)_2]$, in both unenriched and 99% ^{15}N-enriched forms, was prepared by a method already reported.[7] CH_2Cl_2 was distilled from P_2O_5; toluene and pyridine were dried over CaH_2; other solvents and reagents were of the highest available purity and were used without further treatment. All reactions were carried out under an argon atmosphere.

NMR Spectroscopy. Spectra were recorded at 248 and 300 K on a Bruker DRX 400 spectrometer equipped with a 5 mm triple-resonance inverse probe with dedicated ^{31}P channel, operating at 400.13 MHz (^1H), 40.55 MHz (^{15}N), 161.98 MHz (^{31}P), 12.65 MHz (^{103}Rh), and 149.21 MHz (^{119}Sn). Two-dimensional $^{15}N-^1H$ and $^{103}Rh-^{31}P$ spectra were obtained using the pulse sequence of Bax, Griffey, and Hawkins.[8] Nitrogen-15 spectra were recorded from (i) cyanoborate (^{15}N-enriched) with delay times based on $^2J(^{15}N-^1H_{trans}) = 21.5$ Hz and (ii) pyridine (natural-abundance ^{15}N) with delay times based on $^2J(^{15}N-^1H) = 10.5$ Hz (pyridine-2,6-H). For (i) a spectral width in f2 (^1H) of 4 ppm and acquisition time of 0.391 s were used, giving a digital resolution of 1.56 Hz/point, and in f1 (^{15}N) a spectral width of 24 ppm and time domain of 512, giving, after zero filling, a digital resolution of 0.95 Hz/point. With a relaxation delay of 1 s and four scans per increment, data collection required 52 min. Acquisition parameters for (ii) were as follows: spectral width in f2, 4 ppm; acquisition time, 0.391 s; digital resolution in f2, 1.56 Hz/point; spectral width in f1, 4 ppm; time domain, 80; digital resolution in f1 after zero filling, 0.16 Hz/point; relaxation delay, 1 s; scans per increment, 560; data collection time, 20 h. Rhodium-103 spectra were recorded without ^1H decoupling using a spectral width in f2 (^{31}P) of 8 ppm and acquisition time of 0.396 s, giving a digital resolution of 1.26 Hz/point, and in f1 (^{103}Rh) a spectral width of 40 ppm (increased to 1100 ppm for the spectrum given with the Supporting Information) and time domain of 256, giving, after zero filling, a digital resolution of 0.49 Hz/point. With a relaxation delay of 1 s and four scans per increment, data collection required 27 min. To eliminate the possibility of a folded signal in f1, spectra were first recorded with a spectral width of 2000 ppm.

Nitrogen-15, rhodium-103, and tin-119 chemical shifts were referenced to the generally accepted standards of nitromethane, $\Xi(^{103}Rh) = 3.16$ MHz, and tetramethyltin, respectively, with positive values to high frequency. The chemical shifts of CH_3NO_2 and $SnMe_4$ (each neat liquid, CD_2Cl_2 external lock, 248 K) correspond to frequencies of 40.560 342 and 149.210 995 MHz, respectively, in a field (9.395 T) in which the protons of TMS (in CD_2Cl_2 at 300 K) resonate at 400.130 020 MHz.

Kinetic Study. Data were obtained by monitoring the intensity of the $^{31}P\{^1H\}$ signal (calibrated against the signal from Me_3PO_4 contained in a capillary), recorded at −25 °C, of $[Rh(NCBPh_3)(H)(SnPh_3)(PPh_3)(4\text{-}Me_2Npy)]$ as a function of time at an elevated temperature (45−60 °C). The measurement time was held constant at 3 min (80 scans) during which period (at −25 °C) the extent of recombination of the reductive elimination products is negligible. In a typical experiment, a solution (0.6 mL) containing $[Rh(NCBPh_3)(H)(SnPh_3)(PPh_3)_2]$ (10 mg, 0.013 M) and 4-Me_2Npy (18 mg, 0.25 M) in CH_2Cl_2/CD_2Cl_2 (9:1) was prepared at room temperature immediately prior to use and transferred to a 5 mm Wilmad NMR tube. Following a measurement (−25 °C), the sample was transferred to a water bath (maintained at a constant temperature in the range 44−60 °C) for an interval of 1 or 2 min and the reaction then quenched in an ice bath (transfer time 1 s) before returning to the cooled NMR probe. A second spectrum was then recorded and the procedure repeated for a total of 5−12 spectra. Although the accuracy of the measurement of the signal intensity was estimated at ±2−5%, the rate data at 44.6 and 49.2 °C were reproducible to within ±1% and at 54.3 °C to ±2%. The temperature of the bath was measured using a Hewlett-Packard 2801A calibrated against a reference Beckmann thermometer.

Table 1. Crystal Data and Structure Refinement Parameters for **1**

empirical formula	$C_{73}H_{61}BNP_2RhSn$
formula weight	1246.65
temperature	293(2) K
wavelength	0.710 69 Å
crystal system	monoclinic
space group	$P2_1/c$
unit cell dimensions	$a = 12.564(4)$ Å, $b = 26.942(4)$ Å, $c = 18.000(3)$ Å, $\alpha = 90°$, $\beta = 92.93(2)°$, $\gamma = 90°$
volume	6085(2) Å^3
Z	4
density (calcd)	1.361 Mg/m^3
absorption coefficient	0.777 mm^{-1}
$F(000)$	2544
crystal size	0.5 × 0.2 × 0.2 mm
θ range for data collection	2.07−19.99°
index ranges	$-12 < h < 12$, $-5 < k < 25$, $-4 < l < 17$
no. of reflections collected	6773
no. of independent reflections	5660 [R(int) = 0.0116]
refinement method	full-matrix least-squares on F^2
data/restraints/parameters	5655/0/746
goodness-of-fit on F^2	1.096
final R indices [$I > 2\sigma(I)$]	R1 = 0.0419, wR2 = 0.1003
R indices (all data)	R1 = 0.0502, wR2 = 0.1120
largest diff peaks	0.551 and −0.330 e Å^{-3}

X-ray Structure Determination. Orange crystals of **1** were grown from a mixture of $[Rh(NCBPh_3)(PPh_3)_3]$ and excess Ph_3SnH in toluene at room temperature. A crystal of dimensions 0.5 × 0.2 × 0.2 mm was mounted in a Lindemann tube under argon and fixed in place using high-vacuum grease. Crystal quality was verified by means of oscillation and Weissenberg photographs before transferring to an Enraf-Nonius CAD4 diffractometer for data collection. A summary of crystal data and structure refinement is given in Table 1, and the atomic coordinates and equivalent isotropic displacement parameters are given in the Supporting Information. Data reduction and empirical absorption corrections were carried out using the programs PROFIT[9] and XTAL,[10] respectively, while the structure was solved by Patterson methods using SHELXS-86[11] and refined on F^2 using SHELXL-93.[12] The phenyl rings were all constrained as regular six-membered rings (with C−C distances of 1.390 Å) during the full-matrix least-squares refinement, with hydrogen positions and anisotropic displacement parameters, U_{ij}, recalculated before each cycle. The position of the hydride, H(1), was placed from the difference Fourier map. Although it refined satisfactorily in this position, the bond lengths and angles associated with H(1) should be interpreted with caution. Some large anisotropic thermal parameters, U_{ij}, were observed for certain phenyl carbon atoms (e.g., C(423), C(424), and C(434)), indicating a possibility of slight disorder. This, however, would not significantly alter the observed geometry of the $SnPh_3$, PPh_3, and $NCBPh_3$ groups.

A mean-plane calculation using the formula $-6.530x + 7.500y + 14.998z = 1.788$ (least-squares plane with x, y, z in crystal coordinates) was carried out for the atoms P(1), P(2), N(1), and H(1).

Results and Discussion

X-ray Crystallographic Study. The structure of **1** consists of discrete molecules of $[Rh(NCBPh_3)(H)(SnPh_3)(PPh_3)_2]$ with four molecules per unit cell. The ORTEP[13] and SCHAKAL[14] diagrams in Figure 1 show the overall stereochemistry and atomic numbering scheme. Selected interatomic distances and

(7) Carlton, L.; Weber, R. *Inorg. Chem.* **1996**, *35*, 5843.
(8) Bax, A.; Griffey, R. H.; Hawkins, B. L. *J. Magn. Reson.* **1983**, *55*, 301.
(9) Strel'tsov, V. A.; Zavodnik, V. E. *Sov. Phys. Crystallogr.* **1989**, *34*, 824.
(10) Hall, S. R., Flack, H. D., Stewart, J. M., Eds. Xtal 3.2 Reference Manual. Universities of Western Australia, Geneva, and Maryland, 1992.
(11) Sheldrick, G. M. *Acta Crystallogr., Sect. A* **1990**, *46*, 467.
(12) Sheldrick, G. M. SHELXL-93. Universität Göttingen, 1993.
(13) (a) Davenport, G.; Hall, S. R.; Dreissig, W. Xtal 3.2 Reference Manual. Universities of Western Australia, Geneva, and Maryland, 1992. (b) Johnson, C. K. *ORTEP*; Report ORNL-3794; Oak Ridge National Laboratory: Oak Ridge, TN, 1970.
(14) Keller, E. SCHAKAL-92. Universität Freiburg, 1992.

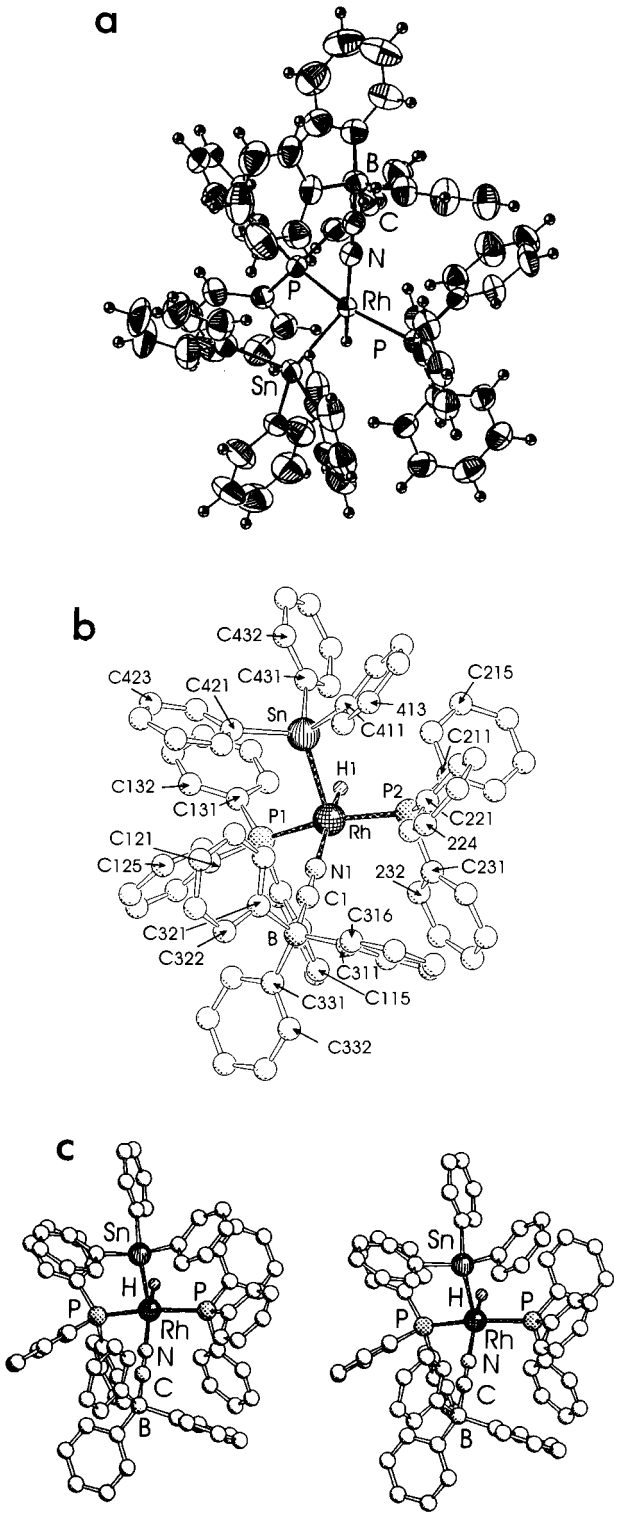

Figure 1. (a) ORTEP drawing of **1** showing thermal ellipsoids at the 50% probability level. (b) SCHAKAL drawing showing the labeling scheme. (c) SCHAKAL stereoview.

interbond angles are listed in Table 2. The geometry about rhodium can conveniently be described as a distorted tetragonal pyramid (or alternatively a distorted trigonal bipyramid) with tin at the apex and rhodium positioned 0.164 Å above the mean plane defined by the hydride, nitrogen and two phosphorus atoms (the corresponding distances for Sn, P(1), P(2), N, and H are 2.515, −0.166, −0.173, 0.119, and 0.220 Å, respectively). The sixth site is blocked by a close interaction between Rh and H(232) (a phenyl hydrogen from P(2)Ph_3), which are positioned

Table 2. Selected Bond Lengths (Å) and Angles (deg) for **1**[a]

Rh−N(1)	2.088(7)	N(1)−C(1)	1.146(8)
Rh−P(1)	2.310(2)	C(1)−B	1.617(10)
Rh−P(2)	2.343(2)	Sn−C(421)	2.158(4)
Rh−Sn	2.559(1)	Sn−C(431)	2.162(4)
Rh−H(1)	1.27(5)	Sn−C(411)	2.168(4)
Sn−H(1)	2.31(5)		
N(1)−Rh−P(1)	92.7(2)	C(131)−P(1)−Rh	119.56(11)
N(1)−Rh−P(2)	91.3(2)	C(111)−P(1)−Rh	102.2(2)
P(1)−Rh−P(2)	162.91(6)	C(221)−P(2)−Rh	123.7(2)
N(1)−Rh−Sn	114.45(14)	C(231)−P(2)−Rh	102.4(2)
P(1)−Rh−Sn	95.66(5)	C(211)−P(2)−Rh	117.8(2)
P(2)−Rh−Sn	97.80(4)	C(1)−B−C(321)	105.3(5)
N(1)−Rh−H(1)	176(2)	C(1)−B−C(331)	107.4(4)
P(1)−Rh−H(1)	92(2)	C(1)−B−C(311)	105.6(4)
P(2)−Rh−H(1)	85(2)	C(421)−Sn−C(431)	104.4(2)
Rh−H(1)−Sn	86(2)	C(421)−Sn−C(411)	103.9(2)
Rh−Sn−H(1)	30(2)	C(431)−Sn−C(411)	104.8(2)
Sn−Rh−H(1)	64(2)	C(421)−Sn−Rh	112.9(1)
C(1)−N(1)−Rh	176.7(5)	C(431)−Sn−Rh	119.7(2)
N(1)−C(1)−B	175.6(7)	C(411)−Sn−Rh	109.7(1)
C(121)−P(1)−Rh	119.9(2)		

[a] All phenyl rings were refined as rigid six-membered rings, with d(C−C) = 1.390 Å.

at a distance of 2.86 Å. A number of (nominally) Rh(III) complexes have been shown to possess such a geometry, viz. (distance from Rh to phenyl hydrogen in parentheses) [Rh(Cl)(CO)(SO_2)(PPh_3)$_2$] (2.94 Å),[15] [Rh(Cl)(H)($SiCl_3$)(PPh_3)$_2$] (2.79 Å),[16] [Rh{PhP($(CH_2)_3PPh_2$)$_2$}(Cl)(N_2Ph)](PF_6) (2.82 Å),[17] [Rh(Cl)($COCH_3$)(PMe_2Ph)$_3$](PF_6) (2.98 Å),[18] and [Rh(Ph)(Cl)$_2$(PPh_3)$_2$] (2.84, 2.86 Å).[19] The geometry about rhodium in **1** is very similar to that found for [Rh(Cl)(H)($SiCl_3$)(PPh_3)$_2$], where the P−Rh−P, H−Rh−Cl, and H−Rh−Si angles are 161.7, 174, and 69°, respectively; the smaller H−Rh−Sn angle of 64° may result from steric repulsion between the bulky triphenyltin and triphenylcyanoborate ligands or from an interaction between tin and hydride, or both. The tin-hydride distance of 2.31(5) Å in **1** compares with 2.02 and 2.16 Å, respectively, in the complexes [Cr($C_6H_3Me_3$)(H)($SnPh_3$)(CO)$_2$][3b] and [Mn(C_5H_4Me)(H)($SnPh_3$)(CO)$_2$],[3a] reported by Schubert et al., where a substantial Sn−H interaction can be inferred. On this basis, the Sn−H interaction in **1** can be regarded as weak but not negligible.

NMR Spin Coupling and Bonding in R_3EH Complexes. The nuclear spin−spin coupling interaction, as originally formulated by Ramsey, is mediated by electrons in the intervening bond(s) and is based on (i) a magnetic dipole−dipole, (ii) an orbital−dipole, and (iii) a Fermi contact interaction (generally considered to be predominant) between the electron and nuclear spins. The magnitude of J is a function of the polarizability of the electron distribution permitted by these interactions (consistent with Pauli's principle) and is related to the energy separation between the ground and an average excited state (ΔE) which governs the extent to which orbital mixing can occur, the average inverse cube of the distance from a valence electron to a coupled nucleus ($\langle r^{-3} \rangle$), the s character of the bond (Fermi contact requires finite electron density at the nucleus), and the magnetogyric ratios of the coupled nuclei in addition to the electron density in the bond (the bond order).[20]

In a simplified description the magnitude of the Sn−H coupling constant in R_3SnH reflects (i) the influence of d orbitals

(15) Muir, K. W.; Ibers, J. A. *Inorg. Chem.* **1969**, *8*, 1921.
(16) Muir, K. W.; Ibers, J. A. *Inorg. Chem.* **1970**, *9*, 440.
(17) Gaughan, A. P.; Ibers, J. A. *Inorg. Chem.* **1975**, *14*, 352.
(18) Bennett, M. A.; Jeffery, J. C.; Robertson, G. B. *Inorg. Chem.* **1981**, *20*, 323.
(19) Fawcett, J.; Holloway, J. H.; Saunders: G. C. *Inorg. Chim. Acta* **1992**, *202*, 111.

on Sn, providing low-lying excited states that are available for mixing with the Sn−H bonding orbital, more readily permitting spin polarization and greatly increasing the absolute value of the Sn−H coupling constant relative to the $^{13}C-^{1}H$ coupling observed for the analogous carbon compounds and (ii) the s character of the Sn−H bond, which is determined by the hybridization of the bonding orbitals (nominally sp^3): with electron-withdrawing substituents on tin the s character of the Sn−H bond increases, while with electron-donating substituents it decreases. These two factors are interrelated. A change in the electron density on tin (as a result of changing one or more substituents) influences not only the s character of the Sn−H bond but also the orbital energies, the effect of electron-withdrawing substituents generally being to increase the average excitation energy (ΔE) so tending to make ^1J(Sn−H) (which has negative sign) less negative, reducing its absolute value. Thus the electron-withdrawing substituent induces two opposing effects: (i) to increase ΔE, causing a reduction in $|J(\text{Sn}-\text{H})|$ and (ii) to increase the s character of the Sn−H bond, leading to an increase in $|J(\text{Sn}-\text{H})|$. It is clear from the fact that $|J(^{119}\text{Sn}-^{1}\text{H})|$ is larger for Ph_3SnH (1950 Hz) than for Bu_3SnH (1578 Hz) that for these compounds the latter is the predominant influence. Factors influencing ^{119}Sn NMR parameters are discussed in a review by Wrackmeyer.[21]

The binding of R_3EH (E = C, Si, Ge, Sn) to a low-valent transition metal complex to form a three-center bonded adduct is considered to occur by two complementary processes: (i) σ activation, involving a transfer of electron density from the E−H σ bond to a vacant orbital of σ symmetry on the metal, and (ii) σ^* activation, in which electron density is transferred from a filled orbital of π symmetry on the metal to the σ^* E−H antibonding orbital, the former being favored by electron-withdrawing substituents on the metal and electron-donating substituents on E, the latter by electron-donating substituents on the metal and electron-withdrawing substituents on E.[22]

Influence of Substituents on Tin. The exchange of Ph_3Sn for Bu_3Sn in complex **1** causes significant changes in a number of NMR spectral parameters (Table 3). The value of $\delta(^{119}\text{Sn})$ increases by more than 200 ppm, J(Sn−H) (further discussion of this parameter will refer to the absolute value) increases by 70%, and J(Rh−Sn) decreases by 30%. By comparison, the complexes $[\text{Rh}(\text{H})\{(\mu\text{-H})\text{SnR}_3\}_2(\text{PPh}_3)_2]$ (R = Ph, Bu) (ref 23 and Table 3) show $\delta(^{119}\text{Sn})$ to increase (by a much smaller amount) and J(Sn−H) and J(Rh−Sn) both to decrease on exchanging Ph for Bu. In other examples of R_3SnH complexes where substituents on tin have been varied, it has been found that as electron-donating substituents are successively replaced by electron-withdrawing substituents the magnitude of J(Sn−H) increases. For example, a study of $[\text{Mo}(\text{Cp})_2(\text{H})(\text{SnR}_3)]$ by Bulychev et al.[24] showed J(Sn−H) to increase from 148 to 314 Hz on replacing Me_3Sn by Cl_3Sn, with similar results obtained from a series of tanlatum complexes,[25] and for the complexes $[\text{Ir}(\text{C}_5\text{Me}_5)(\text{H})_3(\text{SnR}_3)]$, Bergman et al.[26] found an increase in J(Sn−H) from 23.6 to 28.2 Hz on replacing Me_3Sn by Ph_3Sn.

Table 3. NMR Spectral Data

complex[a]	$\delta(^1\text{H})$[b]	$\delta(^{15}\text{N})$[c]	$\delta(^{31}\text{P})$[d]	$\delta(^{103}\text{Rh})$[e]	$\delta(^{119}\text{Sn})$[f]	J(N−H)[g]	J(P−H)	J(Rh−H)	J(Sn−H)[h]	J(P−N)	J(Rh−N)	J(Rh−P)	J(Sn−P)[i]	J(Rh−Sn)
[Rh(NCBPh$_3$)(H)(SnPh$_3$)(PPh$_3$)$_2$] (**1**)[j]	−15.42	−174.8	37.75	120	14.3	16.0	15.9	9.9	29	3.1	15.3	111.1	104	396
[Rh(NCBPh$_3$)(H)(SnBu$_3$)(PPh$_3$)$_2$][k]	−15.79	−172.7	44.26	−132	239.7	16.5	14.8	11.7	50	3.0	15.2	119.2	87	262
trans-[Rh(NCBPh$_3$)(H)(SnPh$_3$)(PPh$_3$)$_2$(py)] (**2a**)	−16.45	−177.9	39.54	512	−148.9	20.3	12.8	10.5	122	2.5	11.8	106.2	155	337
trans-[Rh(NCBPh$_3$)(H)(SnPh$_3$)(PPh$_3$)$_2$(4-Me$_2$Npy)] (**2b**)	−16.44	−177.2	40.25	519	−148.9	20.4	13.1	10.6	125	2.5	11.4	105.9	159	336
trans-[Rh(NCBPh$_3$)(H)(SnPh$_3$)(PPh$_3$)$_2$(4-MeO$_2$Cpy)] (**2c**)	−16.41	−178.3	39.07	510	−146.7	19.6	12.7	10.3	119	2.4	12.4	106.3	156	333
cis-[Rh(NCBPh$_3$)(H)(SnPh$_3$)(PPh$_3$)$_2$(4-Me$_2$Npy)] (**3**)	−16.34	−178.2	36.51	328	64.0	20.6	<1	14.4	92	2.6	11.3	114.4	2380	484
			24.26				22.2			1.6		82.2[l]	160	
cis-[Rh(NCBPh$_3$)(H)(SnPh$_3$)(PPh$_3$)(4-Me$_2$Npy)$_2$] (**4**)	−16.98	−164.1	33.62	1026		22.1	14.1	16.5	167		10.7	82.9	∼130	
trans-[Rh(NCBPh$_3$)(H)(SnPh$_3$)(PPh$_3$)(4-Me$_2$Npy)$_2$] (**5**)	−15.86	−164.9	36.35	1159	92.5	20.8	2.9	16.9	140	2.5	11.5	121.3	2729[m]	507
[Rh(NCBPh$_3$)(H)(SnPh$_3$)(PPh$_3$)(py)] (**6a**)	−16.31	−162.2	54.08	1184	−120.4	22.6	22.7	15.1	99	1.6	12.3	134.6	211	361
[Rh(NCBPh$_3$)(H)(SnPh$_3$)(PPh$_3$)(4-Me$_2$Npy)] (**6b**)	−16.39	−161.3	54.01	1204	−128.9	22.7	22.7	15.5	106	1.6	11.1	132.6	220	367
[Rh(NCBPh$_3$)(H)(SnPh$_3$)(PPh$_3$)(4-MeO$_2$Cpy)] (**6c**)	−16.34	−162.4	54.20	1171	−115.9	22.3	22.7	15.5	95	1.7	11.8	135.3	205	355
[Rh(H)$\{(\mu$-H)SnPh$_3\}_2$(PPh$_3$)$_2$][n]	−7.60		37.6		−58.4		26.1	11.9	170			99.6	17	148.5
[Rh(H)$\{(\mu$-H)SnBu$_3\}_2$(PPh$_3$)$_2$][o]	−9.18		43.26	−1440	−7.7		27.3	14.1	126			103.2	<1	103.4

[a] Solution (0.010−0.020 M) in CD_2Cl_2/CH_2Cl_2 at 248 K unless otherwise specified. Complexes containing pyridine or substituted pyridines (L) were prepared in situ from **1** and L (0.25 M). [b] Chemical shifts in ppm from TMS (internal standard). [c] Chemical shifts in ppm from CH_3NO_2 (external standard). [d] Chemical shifts in ppm from a frequency defined by H_3PO_4 (external standard) *at 300 K*. [e] Chemical shifts in ppm from $\Xi = 3.16$ MHz. [f] Chemical shifts in ppm from $SnMe_4$ (external standard). [g] Coupling constants (absolute magnitude) in Hz. [h] $J(^{119}\text{Sn}-^{1}\text{H}) \approx J(^{117}\text{Sn}-^{1}\text{H})$. [i] $J(^{119}\text{Sn}-^{31}\text{P})$ measured from the ^{119}Sn spectrum. The value for **4** was measured from the ^{31}P spectrum. [j] Chemical shifts (ppm) in dichloromethane at 300 K: −15.53 (H), −174.1 (N), 37.42 (P), 158 (Rh), 11.1 (Sn). [k] Prepared in situ from [Rh(NCBPh$_3$)(PPh$_3$)$_3$] and ^{n}Bu$_3$SnH. Chemical shifts (ppm) in dichloromethane at 300 K: −15.99 (H), −171.9 (N), −43.21 (P), −82 (Rh), 235.9 (Sn). The apparent change in δ(N) on raising the temperature is largely due to the change in δ (0.91 ppm) of the CH_3NO_2 reference. [l] J(P−P) = 20.8 Hz. [m] $J(^{117}\text{Sn}-^{31}\text{P}) = 2608$ Hz measured from the ^{31}P spectrum. [n] Solution in toluene at 295 K (data taken from ref 23). At 248 K, signals other than those of ^{31}P are broadened. The ^{103}Rh signal cannot be detected. [o] Prepared in situ from [Rh(H)(PPh$_3$)$_4$] and ^{n}Bu$_3$SnH. J(P−H), J(Rh−H), and J(Sn−H) were measured at 300 K, at which the ^{1}H signal is well resolved. Chemical shifts (ppm) in toluene at 295 K: −8.85 (H), 42.9 (P), −11.7 (Sn) (data taken from ref 23).

(20) (a) Gutowsky, H. S.; McCall, D. W.; Slichter, C. P. *J. Chem. Phys.* **1953**, *21*, 279. (b) Pople, J. A.; McIver, J. W.; Ostlund, N. S. *J. Chem. Phys.* **1968**, *49*, 2965. (c) Maciel, G. E.; McIver, J. W.; Ostlund, N. S.; Pople, J. A. *J. Am. Chem. Soc.* **1970**, *92*, 1, 11.

(21) Wrackmeyer, B. *Annu. Rep. NMR Spectrosc.* **1985**, *16*, 73.

(22) (a) Saillard, J.-Y.; Hoffmann, R. *J. Am. Chem. Soc.* **1984**, *106*, 2006. (b) Fitzpatrick, N. J.; McGinn, M. A. *J. Chem. Soc., Dalton Trans.* **1985**, 1637. (c) Lichtenberger, D. L.; Kellogg, G. E. *J. Am. Chem. Soc.* **1986**, *108*, 2560. (d) Rabaâ, H.; Saillard, J.-Y.; Schubert, U. *J. Organomet. Chem.* **1987**, *330*, 397.

(23) Carlton, L.; Weber, R. *Inorg. Chem.* **1993**, *32*, 4169.

(24) Protsky, A. N.; Bulychev, B. M.; Soloveichik, G. L.; Belsky, V. K. *Inorg. Chim. Acta* **1986**, *115*, 121.

The anomalous value of J(Sn−H) for [Rh(NCBPh$_3$)(H)(SnBu$_3$)(PPh$_3$)$_2$] compared with that for the SnPh$_3$ analogue can be rationalized as follows: (i) the effects of the lowering of ΔE (arising from the replacement of phenyl by butyl substituents) outweigh the effects of the simultaneous lowering of the s character of the Sn−H bond; (ii) there is an increased (but still weak) interaction between tin and hydrogen. The fact that δ(^{119}Sn) for this complex is at much higher frequency than that for the phenyl analogue suggests that (i) is likely to be the more accurate explanation (the chemical shift is also a function of ΔE).

Reaction of 1 with Pyridines. With pyridine and substituted pyridines in dichloromethane or toluene at −25 °C, **1** reacts to give a colorless solution containing *trans*-[Rh(NCBPh$_3$)(H)(SnPh$_3$)(PPh$_3$)$_2$(L)] (**2a**−**c**) (L = (**a**) py, (**b**) 4-Me$_2$Npy, (**c**) 4-MeO$_2$Cpy) as the only product. The geometry is confirmed by (i) the ^{31}P{^{1}H} spectrum, which consists of a doublet with tin satellites (Figure 2a), (ii) the ^{1}H (Figure 2b,c) and ^{15}N{^{1}H} and ^{119}Sn{^{1}H} (Figure 2g) spectra in which the signals show coupling to two equivalent ^{31}P nuclei, and (iii) the magnitudes of J(Sn−P) and J(N−H)[7,27] (Table 3), which are characteristic of cis and trans couplings, respectively. The binding of pyridine to the vacant site trans to tin causes a shift to high frequency of δ(^{31}P) and δ(^{103}Rh), a shift to low frequency of δ ^{1}H, δ(^{15}N), and δ(^{119}Sn) and an increase in J(Sn−H) by a factor greater than 4. Changes in other coupling constants are much smaller, with J(Sn−P) increasing by ∼60% and other changes being within ±20%. In the series of pyridines L, the substituent in the 4-position is altered so as to influence the nucleophilicity with minimum change in steric properties on complexation: the groups NMe$_2$ and CO$_2$Me occupy positions at opposite ends of the Hammett scale of electron-donating and -withdrawing properties, with H defining the zero point.[28] In the series **2a**−**c** the nuclei N, P, and Rh experience deshielding as the pyridine becomes more nucleophilic, Sn becomes more shielded, and the magnitude of J(Sn−H) increases from 119 to 125 Hz. The compounds are temperature sensitive and within 2 min at 20 °C have undergone further reaction to give, in the case of **2b**, a number of products, some showing similar temperature sensitivities.

Within 1 h of standing at −25 °C, a solution containing **2b** and excess 4-Me$_2$Npy gives a ^{31}P{^{1}H} spectrum (Figure 2a) showing the formation of further products (Scheme 1); these are not observed under the same conditions with L = py or 4-MeO$_2$Cpy. Spectral data (Table 3) are consistent with the formation of *cis*-[Rh(NCBPh$_3$)(H)(SnPh$_3$)(PPh$_3$)$_2$(4-Me$_2$Npy)] (**3**) and *cis*-[Rh(NCBPh$_3$)(H)(SnPh$_3$)(PPh$_3$)(4-Me$_2$Npy)$_2$] (**4**). The ^{31}P{^{1}H} spectrum of **3** contains two signals (each a doublet of doublets with ^{31}P−^{31}P and ^{103}Rh−^{31}P coupling), indicating nonequivalent phosphine environments, i.e. a cis geometry, while J(N−H) indicates N to be positioned trans to H. Complex **4** contains a single phosphine (shown by the coupling pattern in the ^{1}H spectrum, Figure 2b,c) positioned cis to tin (confirmed by J(Sn−P)) and also has N trans to H. When the temperature is raised to 20 °C for 1 min (followed by cooling to −25 °C), a ^{31}P{^{1}H} spectrum (Figure 2d) is obtained which indicates the presence of *trans*-[Rh(NCBPh$_3$)(H)(SnPh$_3$)(PPh$_3$)(4-Me$_2$Npy)$_2$] (**5**) as the major product together with some [Rh(NCBPh$_3$)(H)(SnPh$_3$)(PPh$_3$)(4-Me$_2$Npy)] (**6b**). When the temperature remains at 20 °C (>10 min), **6b** becomes the major product. The geometry of **5** is confirmed by the large value of J(Sn−P), indicating that the phosphine is positioned trans to tin, and J(N−H), which again indicates a trans N−H orientation. The product **6** is also formed with L = py (**a**) and 4-MeO$_2$Cpy (**c**), but with these ligands the intervening products (i.e. **3**−**5**) are not readily detected.

The coordination geometry of **6a** is established unambiguously as that shown in Scheme 1 (it is assumed that the geometries of **6a** and **6b** do not differ greatly) on the basis of

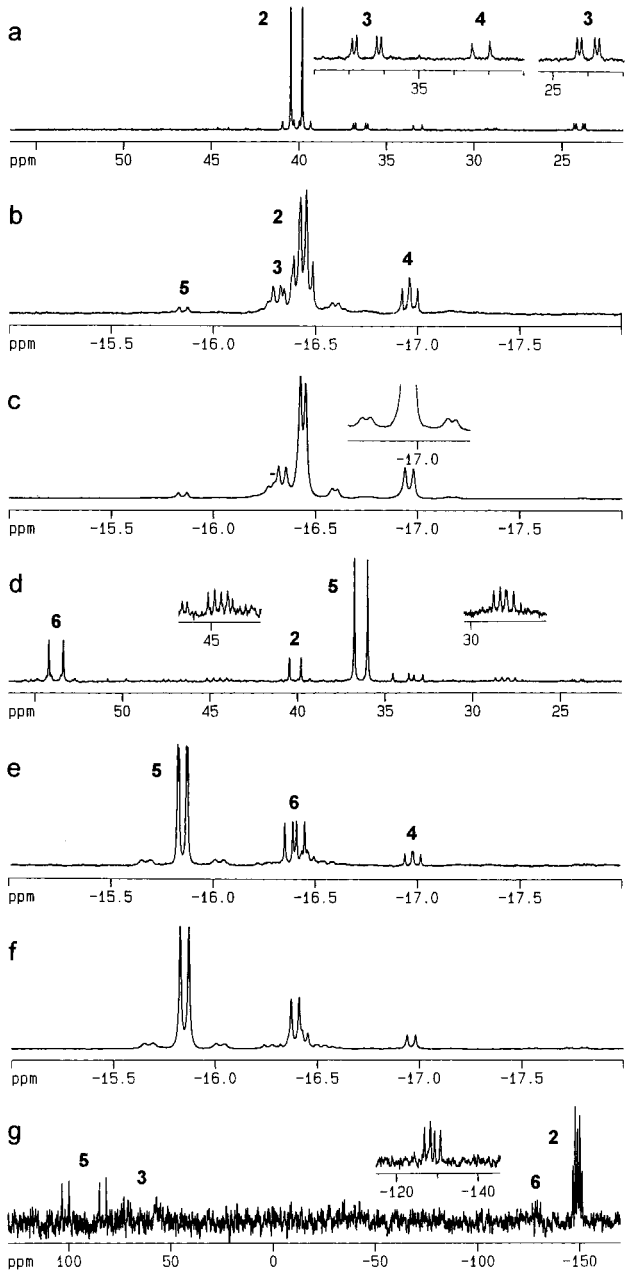

Figure 2. ^{31}P{^{1}H} (a), ^{1}H (b), and ^{1}H{^{31}P} (c) spectra recorded at −25 °C from a mixture of [Rh(NCBPh$_3$)(H)(SnPh$_3$)(PPh$_3$)$_2$] (**1**) (0.025 M) and 4-Me$_2$Npy (0.25 M) in dichloromethane (prepared at <−25 °C). After the mixture was warmed to 20 °C for 1 min, ^{31}P{^{1}H} (d), ^{1}H (e), ^{1}H{^{31}P} (f), and ^{119}Sn{^{1}H} (g) spectra (−25 °C) were obtained. Vertically expanded regions show weak signals (a), tin satellites (c, d), and the signal from 6b obtained from another spectrum (g). Compounds are identified using the scheme defined in the text.

(25) Arkhireeva, T. M.; Bulychev, B. M.; Protsky, A. N.; Soloveichik, G. L.; Belsky, V. K. *J. Organomet. Chem.* **1986**, *317*, 33.
(26) Gilbert, T. M.; Hollander, F. J.; Bergman, R. G. *J. Am. Chem. Soc.* **1985**, *107*, 3508.
(27) (a) Carlton, L.; Belciug, M.-P. *J. Organomet. Chem.* **1989**, *378*, 469. (b) Carlton, L.; de Sousa, G. *Polyhedron* **1993**, *12*, 1377.
(28) (a) Jaffé, H. H. *Chem. Rev. (Washington, D.C.)* **1953**, *53*, 191. (b) Wells, P. R. *Chem. Rev. (Washington, D.C.)* **1963**, *63*, 171. (c) McDaniel, D. H.; Brown, H. C. *J. Org. Chem.* **1958**, *23*, 420.

Scheme 1[a]

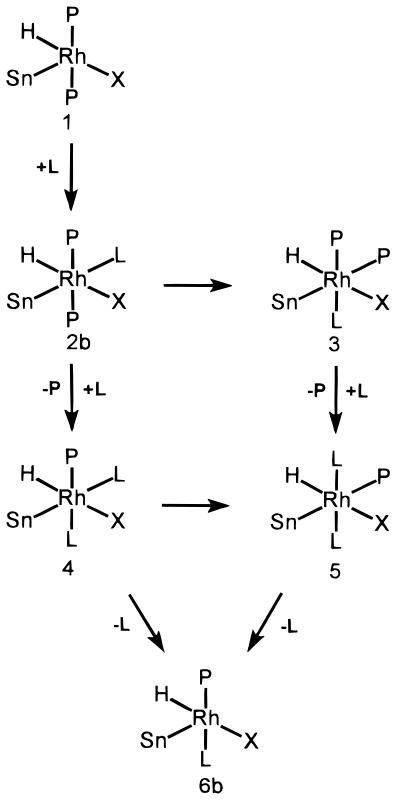

[a] X = $NCBPh_3$, Sn = $SnPh_3$, P = PPh_3, L = 4-Me_2Npy.

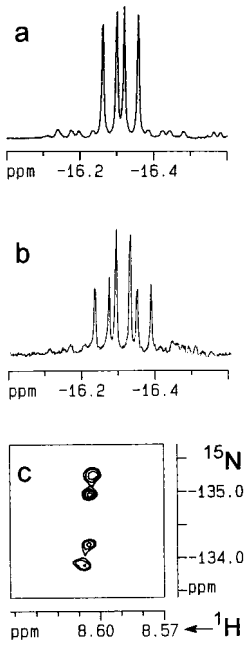

Figure 3. ^{1}H (a, b) and ^{15}N−^{1}H (c) spectra recorded from a mixture of **1** (0.025 M) and pyridine (0.4 M) in C_6D_6 at 27 °C giving [Rh(NCBPh$_3$)(H)(SnPh$_3$)(PPh$_3$)(py)] (**6a**). For spectrum b ^{15}N-enriched **1** was used. Spectrum c shows the signal obtained from the pyridine nitrogen (natural abundance).

(i) the signal from the hydride, which shows coupling to rhodium, to tin, and to only one phosphorus (Figure 3a), (ii) J(N−H) = 22.8 Hz (trans coupling) measured from the ^{1}H spectrum of the ^{15}N-enriched complex (Figure 3b), and (iii) the presence of only one signal from coordinated pyridine in the natural-abundance ^{15}N−^{1}H spectrum, the magnitude of the P−N coupling indicating a trans geometry {δ(^{15}N) −134.7 ppm; J(P−N_{trans}) 43 Hz; J(Rh−N) 12 Hz} (Figure 3c). The pyridine nitrogen of **6b** did not give a clear ^{15}N signal.

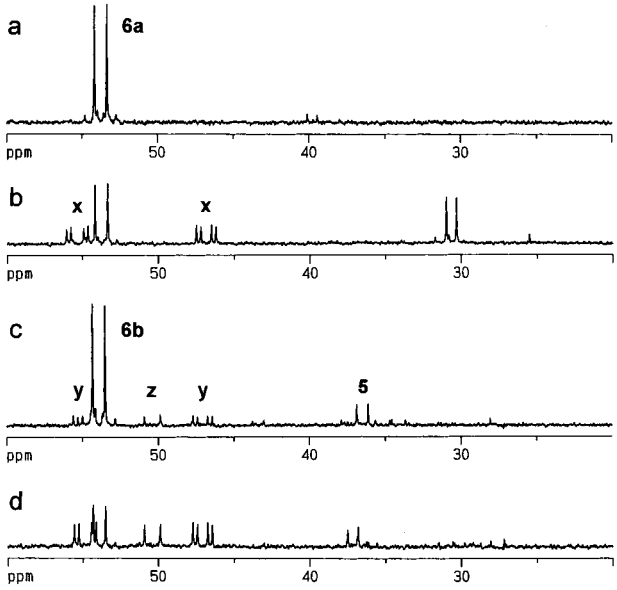

Figure 4. ^{31}P{^{1}H} spectra (∼1000 scans) recorded from solutions containing **1** (0.013 M) and (a, b) py (0.25 M) in toluene and (c, d) 4-Me_2Npy (0.25 M) in 3:2 dichloromethane/toluene at −25 °C after heating at 50 °C for 1 min (a, c), 26 min (b), and 13 min (d). Products *cis*-[Rh(NCBPh$_3$)(PPh$_3$)$_2$(py)], *cis*-[Rh(NCBPh$_3$)(PPh$_3$)$_2$(4-Me_2Npy)], and [Rh(CN)(PPh$_3$)$_2$(4-Me_2Npy)$_2$] are marked x, y, and z, respectively.

Values of J(Sn−H) for **2b**−**6b** were obtained from ^{1}H{^{31}P} spectra shown in Figure 2c,f. From similar spectra (not shown) of the 99% ^{15}N-enriched complexes, values of J(N−H) were measured and used to optimize the pulse sequence for indirect detection of ^{15}N. The ^{15}N and ^{103}Rh chemical shift data were given by ^{15}N−^{1}H and ^{103}Rh−^{31}P HMQC spectra which are included in the Supporting Information. The assignments of ^{1}H and ^{31}P signals were confirmed by ^{31}P−^{1}H correlated spectra (not shown). The positions of the cross peaks corresponding to the tin satellites in the ^{31}P−^{1}H spectra of both **1** and **6a** indicate that J(Sn−P) and J(Sn−H) have the same sign (the high-frequency satellites in the ^{31}P dimension correlate with the high-frequency satellites in the ^{1}H dimension). While these findings give no information about the sign of J, it would appear most unlikely, in view of the similar coordination geometries of **1** and **6a**, that the signs of *both* coupling constants have changed on going from **1** to **6a**. The signs of J(Sn−H) for the two compounds should therefore be regarded as being the same.

Thermal Stability of 1 and 6. On gentle heating (≥35 °C) in dichloromethane or toluene, **6**, prepared in situ from **1** and L, undergoes reductive elimination of Ph_3SnH to give, in the presence of free PPh_3 released by **1** in the reaction with L, *cis*-[Rh(NCBPh$_3$)(PPh$_3$)$_2$(L)] (this compound is reported in ref 7), as shown by the ^{31}P{^{1}H} spectrum in Figure 4a,b. The low solubility of both **1** and 4-Me_2Npy in toluene necessitates the use of dichloromethane or dichloromethane/toluene mixtures. With L = 4-Me_2Npy (but not with pyridine), a second product identified as [Rh(CN)(PPh$_3$)$_2$(L)$_2$] is formed (giving a doublet at δ 50.19 ppm, J(Rh−P) 171.7 Hz, in the ^{31}P spectrum recorded from a solution in dichloromethane at 300 K and a singlet, δ −119.4 ppm, in the ^{15}N spectrum recorded at 248 K). This compound is also formed from [Rh(X)(PPh$_3$)$_3$] (X = CN, $NCBPh_3$) in the presence of 4-Me_2Npy. The reaction is conveniently monitored by ^{31}P{^{1}H} NMR, which shows a

decrease in the intensity of the signal from **6** and the appearance of new signals from the reductive elimination products (Figure 4).

The ^{31}P spectra recorded from warmed solutions of **6a** or **6c** show the formation of another product giving a signal at δ 30.13 ppm (a doublet, J(Rh−P) 109.5 Hz, shown in Figure 4b). This product (which retains the cyanoborate ligand) gives a hydride signal (δ −17.02 ppm) in the ^{1}H spectrum, showing coupling to two ^{31}P nuclei and *two* tins and is evidently formed by the reaction of **6a,c** with the Ph_3SnH liberated by the reductive elimination. This clearly complicates the picture regarding the measurement of a rate of reductive elimination, and data are therefore reported only for experiments using **6b**, in which this product is not formed in significant quantity (Figure 4d). A small amount of **5** is present throughout the experiment, decaying at a rate similar to that observed for **6b**, suggesting that the two are in equilibrium. If this is the case, the presence of **5** should not influence the rate for **6**. During the experiment, the slow growth of a signal (doublet, δ 37.07 ppm, J 112.0 Hz) from an unidentified product (Figure 4d) is also observed. It is possible that these effects may introduce a small to moderate error in the measured rate for the reaction.

Kinetic data for the reductive elimination of Ph_3SnH from **6b** (prepared from **1** (0.013 M) and 4-Me_2Npy (0.25 M) in dichloromethane at 49.2 °C) are consistent with a simple first-order process and not highly dependent on other species in solution. The reaction shows a small to moderate acceleration upon addition of PPh_3 (an 80% increase in rate on raising the concentration from 0.013 to 0.14 M) and 4-Me_2Npy (a 27% increase on raising the concentration to 1.0 M). In view of the generally accepted rule that in the great majority of cases reductive elimination occurs from 16-electron 5-coordinate rather than 18-electron 6-coordinate complexes, these findings can be accounted for in terms of stabilization of the reduced metal fragment[29] formed from **6b**. This interpretation is supported by the observation that in the case of L = MeO_2-Cpy, where addition of PPh_3 converts the 5-coordinate **6c** to 6-coordinate **2c**, the rate of decomposition of **2c** decreases as a linear function of phosphine concentration. The effect of change of solvent (from dichloromethane to toluene) on the rate of reaction for **6c** was found to be a decrease of no more than 30%.

Values of the rate constant (k) measured at 44.6, 49.2, 54.3, and 59.8 °C (0.81×10^{-3}, 1.46×10^{-3}, 2.48×10^{-3}, and 4.46×10^{-3} s^{-1}, respectively) were used in a plot (see Supporting Information) of $\ln(kh/k_BT)$ against T^{-},[1] where h and k_B are the Planck and Boltzmann constants, respectively, to determine $\Delta H^{\ddagger}$ and $\Delta S^{\ddagger}$. The value of $\Delta H^{\ddagger}$ was found to be 97 ± 3 kJ mol^{-1}, measured from the plot, but more realistic error limits, taking into account factors described above, may be ±6 kJ mol^{-1}. The magnitude of $\Delta H^{\ddagger}$ indicates a weak interaction between Ph_3-SnH and rhodium, which, in view of the structurally characterized precedents,[3] is best described as a three-center bond. The Ph_3SnH−Rh interaction is much weaker than that in complex **1**, which is quite stable in solution at 50 °C (with or without added PPh_3) and requires temperatures of at least 85 °C before dissociation of Ph_3SnH will occur. Reductive elimination from **1** is accompanied by rearrangement of the triphenylcyanoborate ligand to the C-bonded form, precluding a meaningful kinetic study. The value of $\Delta S^{\ddagger}$ (1 ± 10 J K^{-1} mol^{-1}, the error limit again more realistically being extended to ± 20 J K^{-1} mol^{-1}) measured for **6b** is not significantly different from zero, suggesting that some internal rearrangement (**6b** is 5-coordinate) may precede dissociation.

In a kinetic study of the replacement of Ph_3SiH by PPh_3 in the complex [Mn(Cp)(H)($SiPh_3$)(CO)$_2$], Hart-Davis and Graham[30] showed the initial step to be the rate-determining dissociation of Ph_3SiH, for which $\Delta H^{\ddagger}$ and $\Delta S^{\ddagger}$ were found to be 122 kJ mol^{-1} and 68 J K^{-1} mol^{-1}, respectively. The presence of a three-center bond in the related complex [Mn($C_5H_4CH_3$)-(H)($SiFPh_2$)(CO)$_2$] was later confirmed by Schubert et al.[6e,f] in a neutron diffraction study.

Trends in NMR Data. The chemical shift of the cyanoborate nitrogen is influenced by changes among the other ligands bound to rhodium: the exchange of a triphenylphosphine of **1** for a pyridine, to give **6a**, is accompanied by a shift to high frequency of 12.6 ppm; the exchange of a phosphine of **3** for 4-Me_2Npy to give **4** likewise causes a change of 14.1 ppm. Similar but much smaller changes are found in the series **2a**−**c** and **6a**−**c** as the pyridine becomes more nucleophilic. These findings are in agreement with those of an earlier study[7] of triphenylcyanoborate complexes of rhodium in which it was found that the ^{15}N chemical shift increases (becomes less negative) with increasing nucleophilicity of the ligands bound to Rh for complexes of the same coordination number. Similar trends have been found for complexes of N_2, CN^{-}, and CO (^{13}C chemical shift).[31]

The rhodium and tin chemical shifts are highly sensitive to changes in the rhodium coordination sphere with increases in δ(^{103}Rh) of 1064 ppm on replacing a PPh_3 of **1** by pyridine to give **6a** and 698 ppm on exchanging a phosphine of **3** for 4-Me_2-Npy to give **4**. By comparison, the complexes [Rh(X)$(H)_2$-$(PPh_3)_3$] (X = O_2CR, SR)[32] have shown increases in δ(^{103}Rh) of ∼400−500 ppm on exchanging PPh_3 for py. The trend in δ(^{103}Rh) resembles, but does not exactly match, that for ^{15}N, with the lowest chemical shift being observed for **1** and the highest for **6**. The ^{119}Sn chemical shift is predictably strongly influenced by the nature of the ligand in the trans position. With pyridine as the trans ligand (complexes **2a**−**c** only—no ^{119}Sn signal could be obtained from **4** because of low concentration), δ(^{119}Sn) has a value of ∼−148 ppm {compared with δ −162.1 ppm (toluene, 22 °C) for uncomplexed Ph_3SnH} increasing to 14.3 ppm for **1** (no trans ligand) and to 92.5 ppm with PPh_3 as the trans ligand (complex **5**). Smaller changes in δ(^{119}Sn) occur in response to variation of the pyridine in complexes **2a**−**c** and **6a**−**c** with increasingly negative values being recorded as the pyridine becomes more nucleophilic.

A comparison of the Sn−H, Sn−P, and Sn−Rh coupling constants for complexes **1** and **6** shows J(Sn−H) to increase by a factor of ∼3, J(Sn−P) also to increase, by a factor of ∼2, and J(Sn−Rh) to decrease by ∼10% on going from **1** to **6**, i.e. on exchanging a phosphine for the more nucleophilic pyridine. By way of contrast, the complex [Rh(H){(μ-H)$SnPh_3$}$_2$(PPh_3)$_2$] gives a high value of J(Sn−H) accompanied by a very low value of J(Sn−P) and low J(Sn−Rh). Values of J(Sn−H) for complexes **1**−**6** increase as the number of pyridine ligands increases (from 0 to 2) and are higher for complexes in which

(29) Suggs, J. W.; Wovkulich, M. J.; Cox, S. D. *Organometallics* **1985**, *4*, 1101.

(30) Hart-Davis, A. J.; Graham, W. A. G. *J. Am. Chem. Soc.* **1971**, *93*, 4388.

(31) (a) Donovan-Mtunzi, S.; Richards, R. L.; Mason, J. *J. Chem. Soc., Dalton Trans.* **1984**, 2429, 2729. (b) Fujihara, T.; Kaizaki, S. *J. Chem. Soc., Dalton Trans.* **1993**, 1275. (c) Toma, H. E.; Vanin, J. A.; Malin, J. M. *Inorg. Chim. Acta* **1979**, *33*, L157. (d) Braterman, P. S.; Milne, D. W.; Randall, E. W.; Rosenberg, E. *J. Chem. Soc., Dalton Trans.* **1973**, 1027. (e) Bodner, G. M.; Todd, L. J. *Inorg. Chem.* **1974**, *13*, 1335. (f) Bodner, G. M.; May, M. P.; McKinney, L. E. *Inorg. Chem.* **1980**, *19*, 1951.

(32) Carlton, L. *Magn. Reson. Chem.* **1997**, *35*, 153.

pyridine, rather than triphenylphosphine, occupies the site trans to tin. The highest value, 167 Hz, observed for **4**, is very similar to that found for $[Rh(H)\{(\mu\text{-}H)SnPh_3\}_2(PPh_3)_2]$. As the nucleophilicity of the pyridine in the two series of complexes **2a**−**c** and **6a**−**c** is increased, a corresponding increase is observed in the magnitude of *J*(Sn−H), a change which is less clearly matched by the other coupling constants listed in Table 3. Thus *J*(Sn−H) appears to reflect changes in electron density on rhodium with greater accuracy than other coupling constants.

Indicators of the Strength of the Three-Center Bond. The effect of replacing a triphenylphosphine of **1** by pyridine (to give **6a**) is to increase $\delta(^{15}N)$ by 12.6 ppm, and $\delta(^{103}Rh)$ by 1064 ppm and to decrease $\delta(^{119}Sn)$ by 134.7 ppm, bringing it closer to the value of −162.1 ppm found for Ph_3SnH. These changes are consistent with an increased electron density on both rhodium and tin. The changes involving tin can be regarded as arising from a weakened interaction of the σ type (see above) where the increased electron density on rhodium causes a decrease in the affinity of Rh for the electron density in the Sn−H bond.

In the series of complexes **1**, **6c**, **6a**, and **6b**, the sequence of increasing ligand nucleophilicity (PPh_3, 4-MeO_2Cpy, py, 4-Me_2Npy) is related to values of $\delta(^{119}Sn)$ of 14.3, −115.9, −120.4, and −128.9 ppm, $\delta(^{103}Rh)$ of 120, 1171, 1184, and 1204 ppm, and $\delta(^{15}N)$ of −174.8, −162.4, −162.2, and −161.3 ppm, respectively. The corresponding values of *J*(Sn−H) are 29, 95, 99, and 106 Hz. The relatively large changes that accompany the increase in electron density on rhodium on exchanging triphenylphosphine for pyridine are matched by smaller variations arising from changes in the nucleophilicity of the pyridine. If the former are associated (as described above) with a weakening of the Rh−H and Rh−Sn bonds and the formation of a Ph_3SnH−Rh three-center bond, it is not unreasonable to conclude that the latter are indicative of smaller, but still significant, changes in the strength of this bond.

Although changes in the overall electron density on rhodium are clearly reflected by a variety of NMR parameters, the average electron density on Rh does not adequately represent the influence on tin of ligands in the trans position. The general rule that electronic influences are transmitted more effectively by trans than by cis ligands is illustrated by the data for complexes **2b** and **3**. The isomers **2b** (pyridine trans to tin) and **3** (phosphine trans to tin) show moderate to small differences in $\delta(^{103}Rh)$ (191 ppm) and $\delta(^{15}N)$ (1.0 ppm) but large differences in $\delta(^{119}Sn)$ and *J*(Sn−H) (changes of 212.9 ppm and 33 Hz, respectively), indicating that while the average electron density on rhodium does not differ greatly for **2b** and **3**, the variation in the ligand trans to tin causes disproportionate changes in the ^{119}Sn NMR parameters which will, to some extent, reflect real changes in Sn−H bonding. These changes, however, will be difficult to quantify on the basis of NMR data alone.

While there is clear evidence that for a series of structurally closely related complexes *J*(Sn−H) is correlated with the strength of the three-center bond, a comparison of values of *J*(Sn−H) for complexes that show greater differences, for example in the identity of the metal, in coordination number, or in the properties of the ligand positioned trans to tin, is less meaningful. Nevertheless it can be said that three-center interactions involving Ph_3SnH may give rise to a tin−hydrogen coupling of no greater than ∼90 Hz. This is a somewhat lower value than hitherto associated with Ph_3SnH−transition metal three-center bonds.

Acknowledgment. We thank the University of the Witwatersrand and the FRD for financial support and Professor H. M. Marques for useful discussions.

Supporting Information Available: Listings of all atomic coordinates, isotropic and anisotropic thermal parameters, and bond lengths and angles for **1** and Figures 5 and 6, showing $^{15}N-^{1}H$ and $^{103}Rh-^{31}P$ HMQC NMR spectra (recorded from **1** and 4-Me_2Npy in dichloromethane at −25 °C; signals in the ^{15}N spectrum are from the cyanoborate nitrogen, enriched to 99%), rate of reaction of **6b** (prepared from **1** and 4-Me_2Npy in dichloromethane) at 49.2 °C to give reductive elimination products, and temperature dependence of the rate (13 pages). Ordering information is given on any current masthead page.

IC970662Y